Proceedings of the World Congress on Engineering and Computer Science 2015 Vol II
WCECS 2015, October 21-23, 2015, San Francisco, USA

Analysis of SOSTTC-OFDM based on Least Squares Method

Oludare Sokoya, *Member, IAENG,* and B.T. Maharaj

***Abstract*—In this paper the error performance of a super-orthogonal space time trellis coded-OFDM system with channel estimation error in a quasi-static frequency selective fading channel is analysed. A least squares estimate of the channel matrix is obtained by using a sequence of pilot symbols. The estimated error is a function of additive white Gaussian noise. The Gauss Chebychev quadrature technique is used to derive the closed form expression of the pairwise error probability (PEP) by assumming the variance of the channel estimation error. Based on the closed form PEP expression, the bit error rate was obtained. Performance results show that the proposed method gives a simulated bit error rate that is correlated with the calculated bit error rate.**

***Index Terms*—Space-time codes, pairwise error probability, OFDM, Gauss Chebychev quadrature technique.**

I. Introduction

SUPER-orthogonal block codes (SOBC) were developed earlier for flat fading [1], [2] (i.e. frequency non-selective fading) channels without temporal interference. In a flat fading channel SOBC in the space and time domain show an improved coding gain and provide full diversity when compared with both space-time block codes [3] and space-time trellis codes [4]. In a frequency selective channel, two main methods can be used to enhance the performance of SOBC, i.e. using of maximum likelihood sequence estimation with multichannel equalisation and Orthogonal Frequency Division Multiplexing (OFDM) where the temporal signal interferences are reduced by converting the frequency selective fading channel into parallel flat fading channels. Two forms of SOBC in the OFDM environment are possible [5]: super-orthogonal space-time trellis coded-OFDM (SOSTTC-OFDM), which is capable of realising both spatial and temporal diversity, and super-orthogonal space-frequency trellis coded-OFDM (SOSFTC-OFDM), which is a scheme that is capable of realising both spatial and frequency diversity. Performance analyses of most coded-OFDM schemes [6], including SOBC-OFDM schemes, have been done based on the assumption that perfect channel estimation is available and that estimation errors are negligible. In spite of the fact that perfect channel estimation is convenient in evaluating the performance of coded-OFDM schemes, performance evaluation when the channel is estimated is a more realistic approach.

Manuscript received July 2, 2015; revised August 7, 2015. This work was supported in part by the Department of Electronic Engineering, Durban University of Technology, South Africa.

O. Sokoya is with the Department of Electronic Engineering, Durban University of Technology, Durban, KZN, 4000 South Africa e-mail: oludares@dut.ac.za.

B. T. Maharaj is the SENTECH Chair in the Broadband Wireless Multimedia Communication Group of the Department of Electrical, Electronic and Computer Engineering, University of Pretoria, Lynnwood, 0002, South Africa e-mail: sunil.maharaj@up.ac.za.

Channel estimation can be performed using two main methods. One is called pilot-based channel estimation [7], [8], which is based on sending training data by the transmitter that is known a priori at the receiver. The other is called blind channel estimation [9], [10], which explores the statistical information of the channel and certain properties of the transmitted signals. Though the blind estimation method has no overhead loss, it is only applicable to slow time-varying channels owing to its need for a long data record and high complexity. Pilot-based channel estimation uses pilot code sequences to estimate the channel. In coded-OFDM and for pilot-based channel estimation, two pilot arrangement methods are possible i.e. block-type or comb-type pilot arrangement.

As a result of the additive noise at the receiver, using pilot based estimation, we apply a least squares based channel estimation technique to SOSTTC-OFDM in a quasi-static frequency selective fading channel. The channel estimation matrix is obtained from the transmitted a priori pilot information at the receiver. A closed form expression of the PEP is derived after the channel has been estimated. The derived PEP is used to calculate the bit error rate and a comparison is made between the calculated and simulated bit error rate.

The paper is organised as described below. Section 2 gives the system model of an SOSTTC-OFDM scheme. The channel estimation technique is presented in Section 3. In Section 4, the authors discuss the performance analysis of the SOSTTC-OFDM, with imperfect channel estimation by using the Gauss Chebychev quadrature technique to determine the closed form expression of the PEP. A numerical example of the PEP using two-state SOSTTC-OFDM is given in Section 5. In Section 6, the PEP obtained in Section 5 is used to calculate the bit error rate and a comparison of both the simulated and calculated bit error rate is made. Some concluding remarks are given Section 7.

II. System Model

An OFDM transmission system with N_t transmit antennas, N_r receive antennas and N subcarriers is considered. The transmission employs concatenating SOSTTC and OFDM as shown in Figure 1.

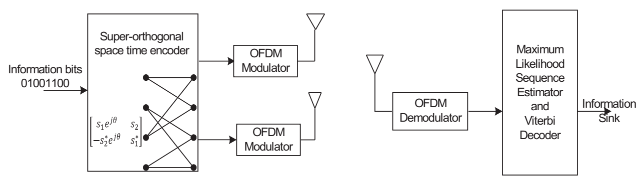

Fig. 1. Transmission diagram for a concatenated SOSTTC and OFDM scheme with $N_t = 2$ and $N_r = 1$.

The super-orthogonal space time trellis encoder is described

ISBN: 978-988-14047-2-5
ISSN: 2078-0958 (Print); ISSN: 2078-0966 (Online)

for $N_t = 2$ (The case of $N_t = 2$ is chosen because for complex orthogonal design, full rate orthogonal block code only exist for $N_t = 2$ [1]). k_c information bits are first mapped into two modulated symbols $\{s_1 \ , \ s_2\}$ and to a rotation angle θ by the trellis encoder related to the current state. The super-orthogonal space time block transmission matrix is given in (1) for $N_t = 2$.

$$A(s_1, s_2, \theta) = \begin{bmatrix} s_1 e^{j\theta} & s_2 \\ -s_2^* e^{j\theta} & s_1^* \end{bmatrix}. \tag{1}$$

The super-orthogonal space time block encoder outputs $s_1 e^{j\theta}$ and $-s_2^* e^{j\theta}$ from the first antenna at the first and second time intervals, respectively. Also on the second antenna, the super-orthogonal space time block encoder outputs s_2 and s_1^*, at the first and second time interval, respectively. For M-phase shift keying (PSK) modulation with a signal constellation represented by $s_i \in e^{j2\pi a/M}, i = 1, 2., a = 0, 1, \cdots, M-1$; one can pick $\theta = 2\pi \acute{a}/M$, where $\acute{a} = 0, 1, \cdots, M-1$. In this case the resulting transmitted signals of (1) are also members of the M-PSK constellation alphabet, and thus no expansion of the constellation signals is required. The choices for θ that can be used in (1), for both binary phase shift keying (BPSK) and quaternary phase shift keying (QPSK), are given as 0, π and 0, $\pi/2$, π, $3\pi/2$, respectively.

It should be noted that when $\theta = 0$, (1) becomes the code presented in [3] (i.e. Alamouti code).

The outputs of the super orthogonal space time encoder from the two antennas can then be transmitted on each OFDM subcarrier. The signal received for an SOSTTC-OFDM scheme, at the jth received antenna, on the nth subcarrier and for two time intervals t and $t+1$, is written as:

$$\begin{bmatrix} r_j^t(n) \\ r_j^{t+1}(n) \end{bmatrix} = \begin{bmatrix} s_1(n)e^{j\theta} & s_2(n) \\ -s_2^*(n)e^{j\theta} & s_1^*(n) \end{bmatrix} \bullet \begin{bmatrix} H_{1j}(n) \\ H_{2j}(n) \end{bmatrix} + \begin{bmatrix} \eta_j^t(n) \\ \eta_j^{t+1}(n) \end{bmatrix}, \tag{2}$$

where $H_{ij}(n)$ is the channel impulse response in the frequency domain from the ith transmit antenna to the jth receive antenna for the nth subcarrier and $\eta_j^t(n)$ is the noise component at the receive antenna j for subcarrier n at time interval t. The noise components are independently identical distributed (i.i.d) complex Gaussian random variables with zero-mean and variance $N_o/2$ per dimension.

Equation (2) can be written in a more compact matrix form for an nth subcarrier, as:

$$\mathbf{r}_j(n) = \mathsf{s}(n)\mathsf{H}_j(n) + \boldsymbol{\eta}_j(n), \tag{3}$$

where $\mathsf{H}_j(n) = [H_{1j}(n) \ H_{2j}(n)]^T$ and for an entire frame of N subcarries, equation (3) can be written as:

$$\mathbf{R}_j = \mathbf{S}\mathbf{H}_j + \tilde{\mathbf{N}}_j, \tag{4}$$

with the individual elements given by,

$$\mathbf{R}_j = [\mathbf{r}_j(1) \ \mathbf{r}_j(2) \ \mathbf{r}_j(3) \ \cdots \ \mathbf{r}_j(N)], \tag{5}$$

$$\mathbf{S} = \begin{bmatrix} \mathsf{s}(1) & 0 & \dots & 0 \\ 0 & \mathsf{s}(2) & \dots & 0 \\ \vdots & \vdots & \ddots & \vdots \\ 0 & 0 & \dots & \mathsf{s}(N) \end{bmatrix}, \tag{6}$$

$$\mathbf{H}_j = [\mathsf{H}_j(1) \ \mathsf{H}_j(2) \ \mathsf{H}_j(3) \ \cdots \ \mathsf{H}_j(N)], \tag{7}$$

and

$$\tilde{\mathbf{N}}_j = [\boldsymbol{\eta}_j(1) \ \boldsymbol{\eta}_j(2) \ \boldsymbol{\eta}_j(3) \ \cdots \ \boldsymbol{\eta}_j(N)]. \tag{8}$$

The time domain channel impulse representation between the ith transmit antenna and the jth receive antenna can be modeled as an L tapped-delay line. The channel response at time t with delay τ_s can be expressed as:

$$h_{ij}(\tau_s, t) = \sum_{l=0}^{L-1} \hat{h}_{ij}(l, t)\delta(\tau_s - n_l/N\Delta f), \tag{9}$$

where $\delta(\cdot)$ is the Dirac delta function, L denotes the number of non-zero taps, $\hat{h}_{ij}(l, t)$ is the complex amplitude of the lth non-zero tap with delay of $n_l/N\Delta f$ (n_l is an integer) and Δf is the tone spacing of the OFDM system. In (9), $\hat{h}_{ij}(l, t))$ is modeled as a wide-sense stationary narrowband complex Gaussian processes with power $E[|\hat{h}_{ij}(l, t))|^2] = \sigma_l^2$, and the normalized channel power: $\Sigma_{l=0}^{L-1}\sigma_l^2 = 1$.

For an OFDM system with adequate cyclic prefix, the channel inpluse response in the frequency domain is expressed as:

$$H_{ij}(n) = \sum_{l=0}^{L-1} \hat{h}_{ij}(l, t)\text{exp}(-j2\pi n(l)/N), \tag{10}$$

where $\hat{h}_{ij}(l, t)$, for $l = 0, 1, 2, \cdots, L-1$, are narrowband zero-mean complex Gaussian processes for the different i transmit antenna and j receive antennas. Equation (10) can be rewritten in matrix form as:

$$H_{ij}(n) = \mathsf{h}_{ij}\mathsf{w}(n), \tag{11}$$

where $\mathsf{h}_{ij} = [\hat{h}_{ij}(0) \ \hat{h}_{ij}(1) \ \cdots \ \hat{h}_{ij}(L-1)]$ is the channel vector, $\mathsf{w}(n) = [w(0) \ w(1) \ \cdots \ w(L-1)]^T$ is the FFT coefficient vector (note that $w(k) = e^{-j2\pi nk/N}$) and T denotes the transpose operation.

III. Channel Estimation

Based on (3), the received signal at the pilot subcarrier p for transmit antenna i and receive antenna j can be written as:

$$\mathbf{r}_j(p) = \mathsf{s}(p)\mathsf{H}_j(p) + \boldsymbol{\eta}_j(p), \tag{12}$$

where $\boldsymbol{\eta}_j(p)$ consist of i.i.d complex Gaussian random noise vectors, $\mathsf{s}(p)$ is the pilot symbols matrix of the form given in (1) and $\mathbf{r}_j(p)$ is the received pilot matix at the pilot instance.

From (12) , the least square estimate [11] of the channel matrix at the pilot subcarrier is given by :

$$\tilde{\mathsf{H}}(p) = \frac{(\mathsf{s}(p))^H \mathbf{r}_j(p)}{\mathsf{s}(p)(\mathsf{s}(p))^H}, \tag{13}$$

where $(\cdot)^H$ denotes the conjugate transpose operator. The pilot symbols must be chosen such that $\mathsf{s}(p)(\mathsf{s}(p))^H$ is invertible. In the remainder of the analysis, the authors will omit the pilot index p in equation (13) for notation convenience.

Using (12) and (13), $\tilde{\mathsf{H}}$ can be rewritten as:

$$\tilde{\mathsf{H}} = \mathsf{H} + \frac{\mathsf{s}^H \boldsymbol{\eta}}{\mathsf{s}\mathsf{s}^H}. \tag{14}$$

ISBN: 978-988-14047-2-5
ISSN: 2078-0958 (Print); ISSN: 2078-0966 (Online)

The denominator in (14) can be written as $\mathsf{ss}^H = N_t\mathbf{I}_{N_t}$, if one assume that all the orthogonal training symbols are selected from a constellation where each member has normalised unit energy, e.g. PSK.
Therefore (14) can be rewriten as:

$$\tilde{\mathsf{H}} = \mathsf{H} + \frac{\mathbf{s}^H\boldsymbol{\eta}}{N_t\mathbf{I}_{N_t}}, \quad (15)$$

The estimate of the channel frequency response written in (15) can be seen to be perturbed by zero mean Gaussian noise and can be rewritten as:

$$\tilde{\mathsf{H}} = \mathsf{H} + \underbrace{\frac{\mathbf{s}^H\boldsymbol{\eta}}{N_t\mathbf{I}_{N_t}}}_{\mathsf{E}} = \mathsf{H} + \mathsf{E}. \quad (16)$$

When the channel frequency response estimate is perfect, the channel frequency estimation error matrix $\mathsf{E} = \mathbf{0}$ and

$$\tilde{\mathsf{H}} = \mathsf{H}. \quad (17)$$

For an entire frame of N transmitted subcarriers the estimated channel frequency response can be expanded as follow:

$$\begin{aligned}\tilde{\mathbf{H}} &= [\tilde{\mathsf{H}}(1) \;\; \tilde{\mathsf{H}}(2) \;\; \tilde{\mathsf{H}}(3) \;\; \cdots \;\; \tilde{\mathsf{H}}(N)] \\ &= [\tilde{\mathsf{h}}_{1j} \;\; \tilde{\mathsf{h}}_{2j}] \bullet \begin{bmatrix} \mathsf{w}(n) & 0 & \dots & 0 \\ 0 & \mathsf{w}(n) & \dots & 0 \\ \dots & \dots & \ddots & \vdots \\ 0 & 0 & \dots & \mathsf{w}(n) \end{bmatrix} \\ &= \tilde{\mathbf{h}}_{ij} \bullet \mathbf{W}(n), \end{aligned} \quad (18)$$

where $\tilde{\mathsf{h}}_{ij} = [\tilde{h}_{ij}(0) \; \tilde{h}_{ij}(1) \; \cdots \; \tilde{h}_{ij}(L-1)]$ is the estimated channel impulse response and $\mathbf{W}(n)$ is the FFT coefficient matrix.
An alternative expression of the estimated channel impulse response as a function of the channel impulse response error $\mathbf{e}$ is written as:

$$\tilde{\mathbf{h}} = \mathbf{h} + \underbrace{\frac{\mathbf{s}^H\boldsymbol{\eta}}{N_t\mathbf{I}_{N_t}\mathsf{w}(n)}}_{\mathsf{e}} = \mathbf{h} + \mathbf{e}. \quad (19)$$

IV. Performance Analysis

To evaluate the performance of the SOSTTC-OFDM system with imperfect channel estimation, the authors use the PEP. The PEP is the probability of choosing the codeword $\hat{\mathbf{S}} = [\hat{\mathsf{s}}(1) \;\; \hat{\mathsf{s}}(2) \;\; \cdots \;\; \hat{\mathsf{s}}(N)]$ when in fact the code $\mathbf{S} = [\mathbf{s}(1) \;\; \mathbf{s}(2) \;\; \cdots \;\; \mathbf{s}(N)]$ was transmitted after the channel has been estimated. The maximum likelihood metric corresponding to the correct path (i.e. $m(\mathbf{R}, \mathbf{S})$) and the incorrect path (i.e. $m(\mathbf{R}, \hat{\mathbf{S}})$) will be used.
The metrics corresponding to the correct and the incorrect paths (i.e. based on (4)) for $j = 1$ are given by (20) and (21) respectively.

$$m(\mathbf{R}, \mathbf{S}) = ||\mathbf{R} - (\tilde{\mathbf{H}}\mathbf{S})||^2, \quad (20)$$

$$m(\mathbf{R}, \hat{\mathbf{S}}) = ||\mathbf{R} - (\tilde{\mathbf{H}}\hat{\mathbf{S}})||^2, \quad (21)$$

where $\tilde{\mathbf{H}}$ is expressed in (18).
The realization of the PEP over the entire frame length and for the estimated channel frequency response is written as:

$$\begin{aligned} P(\mathbf{S} \to \hat{\mathbf{S}}|\tilde{\mathbf{H}}) &= Pr\{m(\mathbf{R}, \mathbf{S}) > m(\mathbf{R}, \hat{\mathbf{S}})\} \\ &= Pr\{(m(\mathbf{R}, \mathbf{S}) - m(\mathbf{R}, \hat{\mathbf{S}})) > 0\} \end{aligned} \quad (22)$$

Simplifying (22) by substituting (20) and (21) gives the following expression:

$$\begin{aligned} P(\mathbf{S} \to \hat{\mathbf{S}}|\tilde{\mathbf{H}}) &= Pr\{||\mathbf{R} - (\tilde{\mathbf{H}}\mathbf{S})||^2) - ||\mathbf{R} - (\tilde{\mathbf{H}}\hat{\mathbf{S}})||^2 > 0\} \\ &= Pr\{||\tilde{\mathbf{H}}\mathbf{S}||^2 - ||\tilde{\mathbf{H}}\hat{\mathbf{S}}||^2 > 0\} \\ &= Pr\{||\tilde{\mathbf{H}}(\mathbf{S} - \hat{\mathbf{S}})||^2 > 0\} \\ &= Pr\{||\tilde{\mathbf{H}}\boldsymbol{\Delta}||^2 > 0\} \end{aligned} \quad (23)$$

where $\boldsymbol{\Delta}$ is the block codeword difference matrix that characterizes the transmitted and erroneous symbols.
The conditional PEP can now be expressed in terms of the complementary error function as:

$$P(\mathbf{S} \to \hat{\mathbf{S}}|\tilde{\mathbf{H}}) = \frac{1}{2}\text{erfc}\left(\sqrt{\frac{E_s}{4N_o}\tilde{\mathbf{H}}\boldsymbol{\Delta}\boldsymbol{\Delta}^H\tilde{\mathbf{H}}^H}\right). \quad (24)$$

Expanding (24) will result in:

$$P(\mathbf{S} \to \hat{\mathbf{S}}|\tilde{\mathbf{h}}) = \frac{1}{2}\text{erfc}\left(\sqrt{\frac{E_s}{4N_o}\sum_{n=1}^{N}\tilde{\mathbf{h}}\Phi(n)(\tilde{\mathbf{h}})^H}\right), \quad (25)$$

where the expression for $\Phi(n)$ is given in (26), $\mathbf{W}(n)$ is given in (18) and $\boldsymbol{\Delta}\boldsymbol{\Delta}^H$ is the codeword difference matrix with detailed expression in (27) and (28).

$$\Phi(n) = \mathbf{W}(n)\Delta(n)(\Delta(n))^H(\mathbf{W}(n))^H, \quad (26)$$

$$\boldsymbol{\Delta}\boldsymbol{\Delta}^H = \begin{bmatrix} \Delta(1)\Delta(1)^H & 0 & \dots & 0 \\ 0 & \ddots & \dots & 0 \\ \vdots & \vdots & \ddots & \vdots \\ 0 & 0 & \dots & \Delta(N)\Delta(N)^H \end{bmatrix}, \quad (27)$$

$$\Delta(n) = \mathsf{s}(n) - \hat{\mathsf{s}}(n). \quad (28)$$

A complementary error function, as defined integrally in [12], is written as:

$$\text{erfc}(b) = \frac{2}{\pi}\int_0^\infty \frac{e^{-b^2(t^2+1)}}{t^2+1}\,dt. \quad (29)$$

The conditional PEP can be expressed as an integral using the above. Thus, with $E(x)$ denoting the average of x, one gets the following expression :

$$\begin{aligned} &\mathsf{P}(\mathbf{S} \to \hat{\mathbf{S}}|\tilde{\mathbf{h}}) \\ &= \frac{1}{\pi}E\left\{\int_0^\infty \frac{\exp[-(t^2+1)\frac{E_s}{4N_o}\sum_{n=1}^{N}\tilde{\mathbf{h}}\Phi(n)(\tilde{\mathbf{h}})^H]}{t^2+1}\,dt\right\}. \end{aligned} \quad (30)$$

The above expression can be simplified further using the results in [13]. For a complex distributed Gaussian random row vector matrix $\mathbf{z}$ with mean $\boldsymbol{\mu}$ and covariance matrix $\sigma_{\mathbf{z}}^2 = E[\mathbf{z}\mathbf{z}^* - \boldsymbol{\mu}\boldsymbol{\mu}^*]$, and a Hermitian matrix $\mathbf{M}$, one can write the expected value as;

$$E[\exp(-\mathbf{z}\mathbf{M}(\mathbf{z}^*)^T)] = \frac{\exp[-\boldsymbol{\mu}\mathbf{M}(\mathbf{I} + \sigma_{\mathbf{z}}^2\mathbf{M})^{-1}(\boldsymbol{\mu}^*)^T]}{\det(\mathbf{I} + \sigma_{\mathbf{z}}^2\mathbf{M})}. \quad (31)$$

ISBN: 978-988-14047-2-5
ISSN: 2078-0958 (Print); ISSN: 2078-0966 (Online)

Based on (31), the mean and variance of the estimated channel impulse matrix needs to be obtained.
As expressed in (19), the estimated channel is a function of the channel impulse response matrix and the channel estimation error. The estimated channel impulse vectors in $\tilde{\mathbf{h}}$ and the channel estimation error vectors in $\mathbf{e}$ are uncorrelated and independent.
The sum of any two independent random variables $\mathrm{X} \sim C(\mu_{\mathrm{X}}, \sigma^2_{\mathrm{X}})$ and $\mathrm{Y} \sim C(\mu_{\mathrm{Y}}, \sigma^2_{\mathrm{Y}})$ that are normally distributed is also normally distributed [14], i.e. ,

$$\begin{aligned} \mathrm{Z} &= \mathrm{X}+\mathrm{Y} \\ \mathrm{Z} &\sim C(\mu_{\mathrm{X}}+\mu_{\mathrm{X}}, \sigma^2_{\mathrm{Y}}+\sigma^2_{\mathrm{Y}}). \end{aligned} \quad (32)$$

Therefore from the above illustration and since the channel impulse responses are zero-mean random variables, the mean of the estimated channel impulse response will be an all-zero matrix while the variance will be the sum of the variance of the channel impulse response matrix and the estimation error matrix. This is expressed as:

$$\sigma^2_{\tilde{\mathbf{h}}} = \sigma^2_{\mathbf{h}} + \sigma^2_{\mathbf{e}} \quad (33)$$

Using (30) and substituting the mean and the variance of the estimated channel, the conditional PEP in (29) can be written as:

$$\begin{aligned} &P(\mathbf{S} \rightarrow \hat{\mathbf{S}}) \\ &= \tfrac{1}{\pi}\int_0^\infty \tfrac{1}{t^2+1}\frac{1}{\det[\mathbf{I}+\frac{E_s}{4N_o}\sigma^2_{\tilde{\mathbf{h}}}\sum_{n=1}^{N}\Phi(n)(t^2+1)]}dt \end{aligned} \quad (34)$$

To solve (34), an integral equation expressed as:

$$I = \frac{1}{\pi}\int_0^\infty \frac{1}{t^2+1} f(t^2+1)dt \quad (35)$$

is considered, where
$f(t^2+1) = \frac{1}{\det[\mathbf{I}+\frac{E_s}{4N_o}\sigma^2_{\tilde{\mathbf{h}}}\sum_{n=1}^{N}\Phi(n)(t^2+1)]}$.
Substituting $y = \frac{1}{t^2+1}$ into (35), leads to the following expression:

$$I = \frac{1}{2\pi}\int_0^1 \frac{1}{\sqrt{y(1-y)}} f(1/y)dy. \quad (36)$$

Equation (36) is in the orthogonal polynomial form of (35) as expressed in [12] and the Gauss-Chebyshev quadrature technique of the first kind can be used to solve it. This may be done as follows:

$$\int_{-1}^{1}\frac{f(u)}{\sqrt{1-u^2}}du = \sum_{i=1}^{m} B_i f(u_i) + \mathrm{V}_m. \quad (37)$$

where $u_i = \cos\frac{(2i-1)}{2m}\pi$, $B_i = \frac{\pi}{m}$ and $\mathrm{V}_m \le \max_{-1<u<+1} \frac{\pi}{(2m)!2^{2m-1}}|f^{2m}(u)|$.
Note that if $2y-1 = u$ then,

$$\begin{aligned} 2y-1 &= \cos\frac{(2i-1)\pi}{2m}, \\ 2y &= \cos\frac{(2i-1)\pi}{2m}+1, \\ \frac{1}{y} &= \sec^2\frac{(2i-1)\pi}{4m}. \end{aligned} \quad (38)$$

Therefore:

$$\begin{aligned} I &= \sum_{i=1}^{m} B_i f(u_i) + \mathrm{V}_m \\ &= \frac{1}{2m}\sum_{i=1}^{m} f\left(\sec^2\frac{(2i-1)\pi}{4m}\right) + \mathrm{V}_m. \end{aligned} \quad (39)$$

The closed form expression of the PEP, using the Gauss Chebyshev quadrature formula as enumerated above, can now be written as follows:

$$\begin{aligned} &P(\mathbf{S} \rightarrow \hat{\mathbf{S}}) \\ &= \tfrac{1}{2m}\sum_{i=1}^{m} \frac{1}{\det[\mathrm{I}+\frac{E_s}{4N_o}\sigma^2_{\tilde{\mathbf{h}}}\sum_{n=1}^{N}\Phi(n)\sec^2\frac{(2i-1)\pi}{4m}]} + \mathrm{V}_m. \end{aligned} \quad (40)$$

As m (which is the order of the polynomial i.e. $f(u_i)$) increases, the remainder term V_m becomes negligible.

V. Numerical Example

As an example, a two-state SOSTTC-OFDM trellis is used. Figure 2a represent the trellis when BPSK symbols are transmitted while Figure 2b represent the trellis when QPSK symbols are transmitted. In the trellises, two sets, each containing two pairs of symbols, are assigned to each state, i.e. there is a pair of parallel paths between each pair of states. The label $(s,l)/A(s_i,s_j,\theta)$ along each branch of the trellises refers to the pair of input symbols (s,l) and the corresponding output symbol function $A(s_i,s_j,\theta)$. For

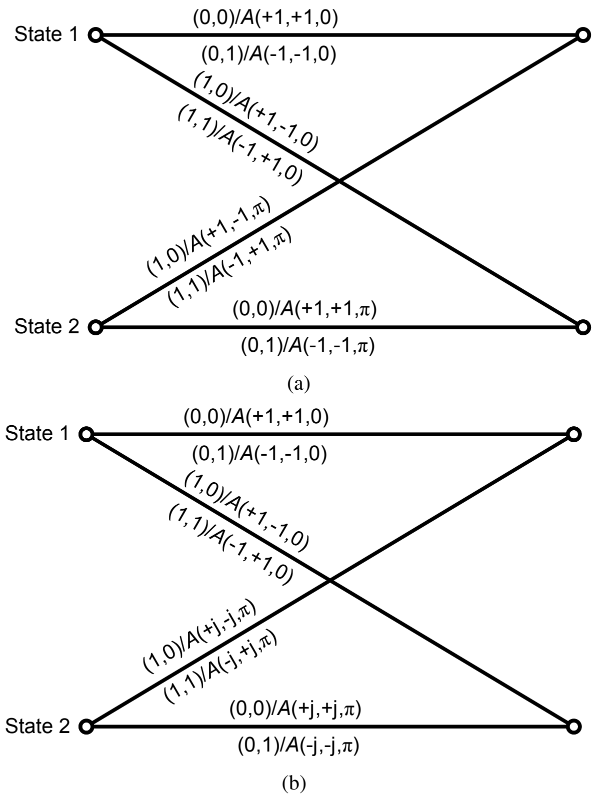

Fig. 2. Two-state SOSTTC-OFDM

$N_t = 2, N_r = 1$ and $L = 2$, the FFT coefficient matrix $\mathbf{W}(n)$ can be written as:

$$\mathbf{W}(n) = \begin{bmatrix} 1 & 0 \\ w(n) & 0 \\ 0 & 1 \\ 0 & w(n) \end{bmatrix}. \quad (41)$$

ISBN: 978-988-14047-2-5
ISSN: 2078-0958 (Print); ISSN: 2078-0966 (Online)

To obtain the pairwise error probability, the error events of the trellises will be considered.
In Figure 2a, the first parallel paths, where $n = 1$, which correspond to an error event length of 1 are considered, i.e. $L_e(1)$. The codeword matrix obtained from the trellis and $\mathbf{W}(n)$ values is written as:

$$L_e(1) = \mathbf{W}(1) \bullet \begin{bmatrix} 2 & -2 \\ 2 & 2 \end{bmatrix} \bullet \begin{bmatrix} 2 & 2 \\ -2 & 2 \end{bmatrix} \bullet (\mathbf{W}(1))^H . \quad (42)$$

For an error event of length 2, i.e. $n = 2$, the codeword matrix obtained from the trellis based on the addition of the dominant error paths is expressed as:

$$L_e(2) = \mathrm{A} + \mathrm{B}, \quad (43)$$

where

$$\mathrm{A} = \mathbf{W}(1) \bullet \begin{bmatrix} 0 & -2 \\ 2 & 0 \end{bmatrix} \bullet \begin{bmatrix} 0 & 2 \\ -2 & 0 \end{bmatrix} \bullet (\mathbf{W}(1))^H, \quad (44)$$

and

$$\mathrm{B} = \mathbf{W}(2) \bullet \begin{bmatrix} 0 & -2 \\ 0 & 2 \end{bmatrix} \bullet \begin{bmatrix} 0 & 0 \\ -2 & 2 \end{bmatrix} \bullet (\mathbf{W}(2))^H \quad (45)$$

For an error event of length 3, the codeword matrix obtained from the trellis based on the addition of the dominant error paths is expressed as:

$$L_e(3) = \mathrm{A} + \mathrm{B} + \mathrm{C}, \quad (46)$$

where

$$\mathrm{A} = \mathbf{W}(1) \bullet \begin{bmatrix} 0 & -2 \\ 2 & 0 \end{bmatrix} \bullet \begin{bmatrix} 0 & 2 \\ -2 & 0 \end{bmatrix} \bullet (\mathbf{W}(1))^H, \quad (47)$$

$$\mathrm{B} = \mathbf{W}(2) \bullet \begin{bmatrix} 0 & 0 \\ 2 & 2 \end{bmatrix} \bullet \begin{bmatrix} 0 & 2 \\ 0 & 2 \end{bmatrix} \bullet (\mathbf{W}(2))^H, \quad (48)$$

and

$$\mathrm{C} = \mathbf{W}(3) \bullet \begin{bmatrix} 0 & -2 \\ 0 & 2 \end{bmatrix} \bullet \begin{bmatrix} 0 & 0 \\ -2 & 2 \end{bmatrix} \bullet (\mathbf{W}(3))^H \quad (49)$$

For other error events in Figures 2a and 2b, the codeword matrices can be calculated with respect to the various error event paths using the above method .
For different SNR, the calculated codeword matrix is then substituted into the closed form PEP equation given in (40). The variance of the estimated channel will be an identity matrix whose diagonal elements is 0.5, since the channel power has been normalised to one. The PEP curves in Figure 3 and Figure 4 are generated based on the assumptions that the remainder value V_m is negligible and the order polynomial equals to 2.
In Figures 3 and 4, the PEP performance of a two state SOSTTC-OFDM code for when BPSK and QPSK symbol are transmitted is shown, respectively. In both Figures, an error event of length 2 has the worst PEP compared to error event of length 1, 3, 4 and 5. This is because for the chosen SOSTTC-OFDM transmission, the dominant error event is concentrated at error event path of length 2. This is the worst case PEP scenario for the code.
Since a BER is of greater importance in digital communication than the PEP, an estimation of the BER for SOSTTC-OFDM with channel estimation error is obtained by accounting for the error event path up to a pre-determined specific

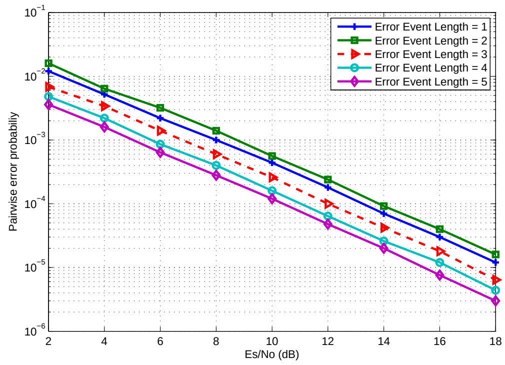

Fig. 3. PEP performance of two-state BPSK SOSTTC-OFDM

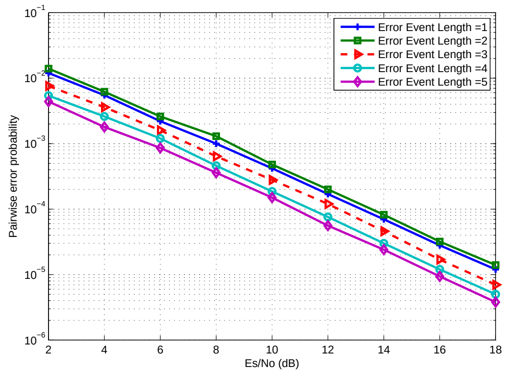

Fig. 4. PEP performance of two-state QPSK SOSTTC-OFDM

value using (50),

$$P_b(E) \approx \frac{1}{b} \sum_{\mathbf{S} \neq \hat{\mathbf{S}}} q(\mathbf{S} \to \hat{\mathbf{S}}) \mathsf{P}(\mathbf{S} \to \hat{\mathbf{S}}). \quad (50)$$

In (50) b is the number of input bits per trellis transition and $q(\mathbf{S} \to \hat{\mathbf{S}})$ is the number of bit errors associated with each error event. If the maximum length of error events taken into account is chosen as L_e, it is sufficient to consider the error event up to L_e. This represents a truncation of the infinite series used in calculating the union bound on the bit error probability for high SNR values. The choice of L_e is critical in the sense that most of the dominant error events for the range of SNRs of interest should be properly chosen to prevent excessive computational complexity (the computational complexity grows exponentially with L_e).
To approximate the BER by considering only the error event path of one, two, three, four and five, the BER_1, BER_2, BER_3,BER_4, and BER_5 respectively, are used.

$$\mathrm{BER}_1 \approx \frac{1}{2}(\mathrm{PEP}_1) \quad (51)$$

$$\mathrm{BER}_2 \approx \frac{1}{2}(\mathrm{PEP}_1 + 12 * \mathrm{PEP}_2) \quad (52)$$

$$\mathrm{BER}_3 \approx \frac{1}{2}(\mathrm{PEP}_1 + 12 * \mathrm{PEP}_2 + 28 * \mathrm{PEP}_3) \quad (53)$$

$$\mathrm{BER}_4 \approx \frac{1}{2}(\mathrm{PEP}_1 + 12 * \mathrm{PEP}_2 + 28 * \mathrm{PEP}_3 + 64 * \mathrm{PEP}_4) \quad (54)$$

ISBN: 978-988-14047-2-5
ISSN: 2078-0958 (Print); ISSN: 2078-0966 (Online)

$$\mathrm{BER}_5 \approx \frac{1}{2}(\mathrm{PEP}_1 + 12 * \mathrm{PEP}_2 + 28 * \mathrm{PEP}_3 + 64 * \mathrm{PEP}_4 + 144 * \mathrm{PEP}_5) \quad (55)$$

The number of errored bits for various error events in Figure 2b, can be enumerated using the above mentioned methods

VI. Performance Result

The simulated and the calculated performance of an SOSTTC-OFDM system in a quasi-static frequency selective fading channel are presented. The same parameter stated is used for the calculated and simulated code. In Figures 5 and 6, the simulated BER for N=64 is compared with the calculated BER for various error events: 1, 2, 3, 4 and 5, which correspond to N = 2, 4, 6, 8 and 10, respectively. The graph shows that an increase in the error events (i.e. from 1 to 5) gives a more accurate and tighter BER evaluation compared with the simulated one. The graph shows that for a maximum error event of length 5, the analysis and the simulation are very close, therefore for the high SNR region, the calculated BER values can be used instead of simulation, which can be time- consuming.

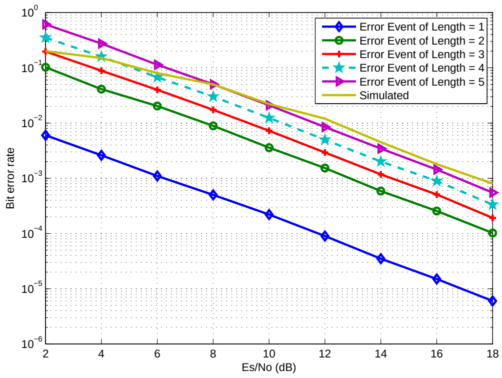

Fig. 5. BER of BPSK SOSTTC-OFDM with channel estimation error.

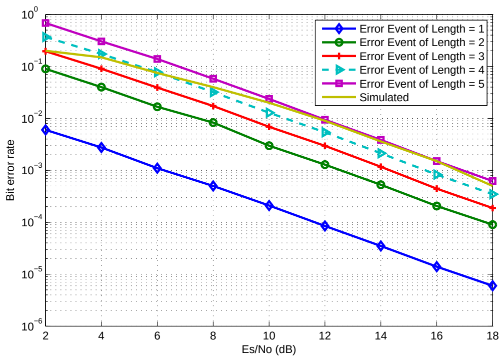

Fig. 6. BER of QPSK SOSTTC-OFDM with channel estimation error.

VII. Conclusion

The analysis of the PEP and BER performance of SOSTTC-OFDM, with channel estimation error in a quasi-static frequency selective fading channel, is considered. By assuming the statistical distribution of the estimation error, a closed form expression for the PEP can be derived. The expression derived is used to calculate the BER. The results presented show that, for high SNR region, the analytical BER and the simulated BER have a tight-bound for an error event of length 5 .

References

[1] H. Jafarkhani and S. Seshadri, “Super-orthogonal space-time trellis codes,” *IEEE Transactions on Information Theory*, vol. 49, pp. 937–950, April 2003.
[2] M. Bale, B. Laska, D. Dunwell, F. Chan, and H. Jafarkhani, “Computer Design of Super-Orthogonal Space-Time Trellis Codes,” *IEEE Transactions on Wireless Communication*, vol. 6, no. 2, pp. 463–467, February 2007.
[3] S. Alamouti, “Space-time block coding: A simple transmitter diversity technique for wireless communications,” *IEEE Journal on Selected Areas in Communication*, vol. 16, pp. 1451–1458, October 1998.
[4] V. Tarokh, H. Jafarkhani, and A. R. Calderbank, “Space-time codes for high data rate wireless communication; Performance analysis and code construction,” *IEEE Transactions on Information Theory*, vol. 44, no. 2, pp. 744–756, March 1998.
[5] O. Sokoya and B. Maharaj, “Super-Orthogonal Block Codes with Multichannel Equalisation and OFDM in Frequency Selective Fading,” *EURASIP Journal on WIreless Communication and Networking*, pp. 1–10, August 2010.
[6] Y. Ma and M. Patzold, “Performance analysis of alamouti coded ofdm systems over rayleigh fading channels correlated in space and time,” in *Vehicular Technology Conference (VTC 2010-Spring), 2010 IEEE 71st*, May 2010, pp. 1–6.
[7] B. C. Chen, W. J. Lin, and J. S. Lin, “Pilot-assisted channel estimation for STBC-based wireless MIMO-OFDM systems,” in *Proceedings of the international conference on Wireless communications and mobile computing*, New York, USA, 2007, pp. 411–416.
[8] G. Jency and S. Gladwin, “Channel estimation using optimized pilot placement in ofdm system,” in *Communications and Signal Processing (ICCSP), 2014 International Conference on*, April 2014, pp. 1529–1534.
[9] W. Bai, “Blind channel estimation in MIMO-OFDM systems,” *IECE Transaction on Communication*, vol. E85-B, no. 9, pp. 1849–1853, October 2002.
[10] S. Yatawatta and A. P. Petropulu, “Blind channel estimation in MIMO-OFDM systems,” in *Proceedings of the IEEE Workshop Statistical Signal Process*, September 2003, pp. 363–366.
[11] M. Biguesh and A. B. Gershman, “Training-Based MIMO Channel Estimation: A study of Estimator Tradeoffs and Optimal Training Signals,” *IEEE Transactions on Signal Processing*, vol. 54, no. 3, pp. 884–893, March 2006.
[12] M. Abramovitz and I. A. Stegun, “Handbook of Mathematic Functions,” *Dover, New York*.
[13] G. L. Turin, “The Characteristic function of Hermetian quadratic forms in complex normal random variables,” *Biometrika*, pp. 199–201, June 1960.
[14] J. Proakis, “Digital Communication,” *McGraw-Hill Higher*, 2000.

Oludare Sokoya received his BSc (Eng) from Obafemi Awolowo University, Nigeria, MSc(Eng) from University of KwaZulu-Natal and a PhD in Electronic Engineering from the University of Pretoria. Dr. Sokoya is currently a Senior lecturer at the Durban University of Technology. His research interests are in advanced physical layer technologies for wireless communication.

B.T. Maharaj received his BSc (Eng) and MSc(Eng) in Electronic Engineering from the University of Natal (Durban). He received an MSc in Operational Telecommunications with merit from the University of Coventry and a PhD in Wireless Communications from the University of Pretoria. Professor Maharaj research interests are in OFDM-MIMO systems and cognitive radio.

ISBN: 978-988-14047-2-5
ISSN: 2078-0958 (Print); ISSN: 2078-0966 (Online)